

# Origin of Embrittlement of Commercial Nuclear Reactor Pressure Vessel Steels: Cu-rich Precipitates and Defects

*Mechanisms of embrittlement of nuclear reactor pressure vessel steels were studied by using positron annihilation spectroscopy combined with 3D atom probe technique. In surveillance test specimens of a commercial western-type pressurized water reactor, Cu precipitation takes place at the very beginning of reactor lifetime, which is followed by formation of irradiation defects.*

The irradiation-induced embrittlement of the nuclear reactor pressure vessel (RPV) steels is currently a vital issue for ensuring safe operation of nuclear power plants in the world since the reactors of the first generation are going to exceed their initially designed operation lifetimes. Thus, it is of great importance to reveal the nanostructural change, attributed to the origins of the embrittlement, during long-term operation of the commercial nuclear reactors [1]. Here we demonstrate the formation of Cu-rich nano-precipitates (CRNPs) at the very beginning of the reactor lifetime by using 3D atom probe (3DAP), which is followed by retarded formation of irradiation defects (matrix defects) by using positron annihilation, in surveillance test specimens of a pressurized water reactor (PWR), Doel-2 in Belgium.

Figure 1 shows 3DAP atom maps of the solute distributions in Doel-2 RPV surveillance test specimens of low dose ((a)  $0.83 \times 10^{19}$  n/cm<sup>2</sup>) and high dose ((b)  $5.1 \times 10^{19}$  n/cm<sup>2</sup>), corresponding to the in-service irradiation periods for about 3 and 20 years, respectively. Local-electrode type 3DAP apparatus was employed, which enabled us to analyze much larger volume than conventional type 3DAP and to reduce the fracture of the irradiated needle specimens. In the both specimens, CRNPs were clearly observed, which shows that 3 years of irradiation is enough to cause Cu precipitation in the reactor, and the coarsening of CRNPs takes place with increasing the dose. In the CRNPs, Mn and P atoms are enriched even at the low dose, while Ni atoms are enriched only at the high dose.

The residual Cu content in the matrix are also obtained from the 3DAP mappings directly. We found that the residual Cu content for the high dose is similar (0.1% in weight) to that for the low dose, showing that the fraction of Cu atoms consisting of CRNPs has saturated at the beginning of the irradiation.

Figure 2 shows high (H)/ low (L) momentum component fractions of coincidence Doppler broadening (CDB) spectra for the Doel-2 surveillance test specimens, normalized to those for pure Fe (unirradiated). The (L,H) points for the well-annealed pure Cu, and neutron-irradiated pure Fe are also plotted as references. Higher L and H correspond to positron trapping at vacancy-type defects and at CRNPs due to positron quantum-dot-like state [2], respectively. The results shows that the vacancy-type defects have accumulated with dose so that the fraction of positrons trapped at the vacancy-type defects increases, accompanying decrease in the annihilation fraction in CRNPs. By positron lifetime method [3], the vacancy-type defects are identified mainly as small vacancy clusters (V<sub>3</sub>-V<sub>4</sub>).

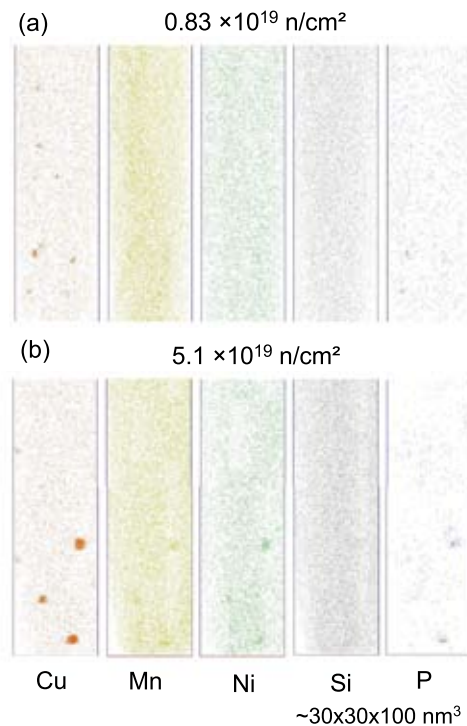


Fig. 1. 3DAP atom maps of the solute distributions in RPV surveillance test specimens of Doel-2. (a)  $0.83 \times 10^{19}$  n/cm<sup>2</sup>, (b)  $5.1 \times 10^{19}$  n/cm<sup>2</sup>.

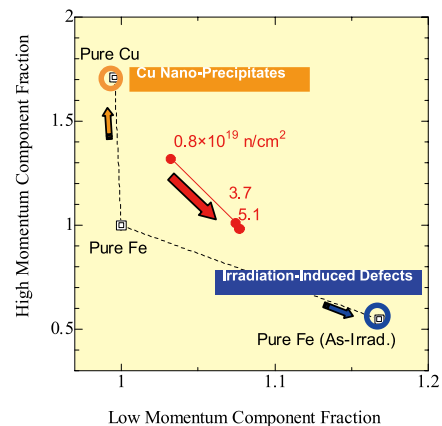


Fig. 2. High/Low momentum component fractions of CDB spectra for Doel-2 surveillance test specimens.

## References

- [1] Y. Nagai et al., Appl. Phys. Lett. **87**, 261920 (2005).
- [2] Y. Nagai et al., Phys. Rev. B. **63**, 134110 (2001).
- [3] M. Jardin et al., Nucl. Instr. Meth. In Phys. Res. A **568**, 716 (2006).

## Contact to

Yasuyoshi Nagai (Irradiation Effects in Nuclear and Their Related Materials Division)  
e-mail: nagai@imr.tohoku.ac.jp

# Electrical Conductivity of Proton Conductive Ceramics under Reactor Irradiation

Electrical charges may be transported in ceramics by not only electrons but also by electron-holes, ions, and protons. Especially in nuclear fusion environments, electrical conductivity by proton migration (protonic conduction) will play an important role, as supply of hydrogen isotopes is sufficient and working temperature for ceramics will be in general high.

Perovskite-type oxides, yttrium doped barium-cerium oxide, ( $\text{BaCe}_{0.9}\text{Y}_{0.1}\text{O}_{3-\delta}$ ), were irradiated in the Japan Materials Testing Reactor (JMTR) in the Oarai Research Establishment of Japan Atomic Energy Agency (JAEA) [1]. The electrical conductivity was measured in-situ under the reactor irradiation, as illustrated in Fig. 1. The fast ( $E > 1.0$  MeV) and the thermal ( $E < 0.683$  eV) neutron fluxes were in the range of  $1 \times 10^{16}$ - $6 \times 10^{17}$  and  $1 \times 10^{17}$ - $1.6 \times 10^{18}$  n/m<sup>2</sup>s, respectively. The associated gamma-ray dose rates were in the range 0.1-2.0 kGy/s. Subcapsules, each of which was containing one specimen, were accommodated in an instrumented rig whose atmosphere was partially circulating purified helium of 2 atmospheric-pressure. The temperature was controlled by electric heaters as well as by changing the helium gas pressure between the subcapsule and the irradiation rig, after the reactor reached its steady-state operation mode at 50 MW [1-3]. The guard-ring configuration was adopted but a guard ring was connected to the ground potential through a wall of the subcapsule accommodating the specimen. Thin zirconium films were deposited on both sides of a disk-like specimen as electrodes and two platinum wires were connected to the two zirconium electrodes working as a cathode and an anode. The guard ring electrode was connected to a stainless-made subcapsule wall through a thick copper made specimen holder which is circumventing a leakage electrical current from coming into a current-measuring-side electrode. To study protonic conductivity, 10keV proton ions were implanted into the anode side zirconium film and oxygen ions into the cathode side.

Figure 2 summarizes temperature dependence of the

electrical conductivity of  $\text{BaCe}_{0.9}\text{Y}_{0.1}\text{O}_{3-\delta}$ . The electrical conductivity could be composed of two mechanisms; one having a lower apparent activation energy of about 0.2 eV (mechanism 1; electron conduction) in the temperature range below 480K, and the other having a higher apparent activation energy of about 0.7-0.8 eV (mechanism 2; proton conduction). The hydrogen implantation into the anode did not alter the electron conductivity substantially but increased the proton conductivity by about the two orders of magnitude. Under JMTR irradiation, measurements of temperature dependence of the electrical conductivity below about 400 K could not be realized due to a large nuclear heating rate and the electrical conductivity by mechanism 1 could not be evaluated during the JMTR steady-state operation. Without the hydrogen implantation into the anode, the increase of the proton conductivity by 2 kGy/s irradiation was about 7 times. In the meantime, with the hydrogen implanted anode, the observed increase of proton conductivity by the 1.1 kGy/s irradiation was more than two orders of magnitude. Under the JMTR irradiation, further increase of the electrical conductivity (mechanism 3) from that by the mechanism 2 was observed at higher temperatures, namely, above 623 K for the specimen without hydrogen and above 523 K for the specimen with hydrogen. This increase of the electrical conductivity at higher temperatures was not observed in the bench top experiments as can be seen in Fig. 2.

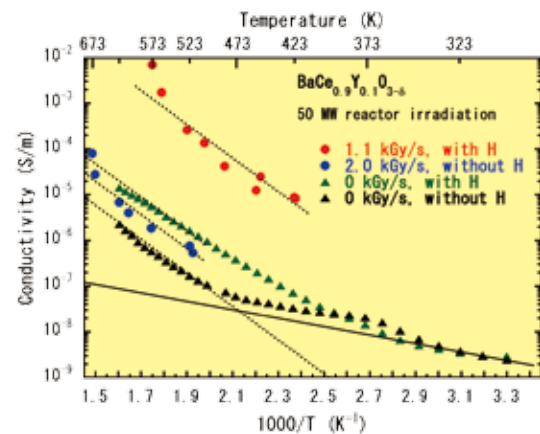


Fig. 2. Temperature dependence of electrical conductivity of  $\text{BaCe}_{0.9}\text{Y}_{0.1}\text{O}_{3-\delta}$ , without irradiation and under JMTR irradiation.

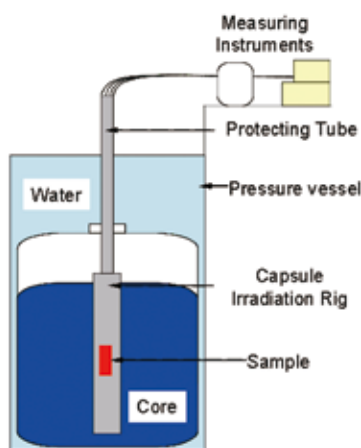


Fig. 1. Schematic of the electrical conductivity in-situ measurement under JMTR irradiation.

## References

- [1] T. Shikama, B. Tsuchiya, S. Nagata and K. Toh, *Advances in Science and Technology* **45**, 1974 (2006).
- [2] B. Tsuchiya, T. Shikama, S. Nagata, K. Toh, M. Narui and M. Yamazaki, *J. Nucl. Mater.* **329-333**, 1511 (2004).
- [3] B. Tsuchiya, S. Nagata, K. Saito, K. Toh and T. Shikama, *Materials Science Forum* **480-481**, 579 (2005).

Contact to

Tatsuo Shikama (Nuclear Materials Science Division)

e-mail: shikama@imr.tohoku.ac.jp

# Quantitative Analysis of the Dependence of Hardening on Copper Precipitate Diameter and Density in Fe-Cu Alloys

*In-situ TEM observations during tensile tests of dislocation gliding through copper precipitates in thermally aged Fe-Cu alloys were performed. The obstacle strength was estimated from the critical bow-out angle,  $\varphi_c$ , of dislocations. A good agreement was obtained between hardening estimation based on the critical bowing angles and those obtained from conventional tensile tests.*

It is well known that the radiation-induced defect clusters in metals are responsible for significant changes in mechanical properties. Examples of extended crystal defect clusters include precipitates, voids, dislocation lines and loops, and so on. Understanding the quantitative effect of such radiation-induced defect clusters on dislocation motion is important for construction of predictive models to estimate the lifetime of power plant components. We investigate the dependence of hardening on copper precipitate diameter and number density by performing in-situ TEM observations during tensile tests in thermally aged Fe-Cu alloys [1,2]. The obstacle strength  $\alpha$  was determined as  $\alpha = \cos(\varphi_c/2)$  at the point of dislocation break away from the obstacle. The critical bow-out angle  $\varphi_c$  was taken as the angle between two tangent lines drawn from the cusp in the line tension approximation. The number density of obstacles was determined from the dislocation segment length  $L$  between two adjacent pinning points. Comparison is made between number densities estimated from in-situ observations and those obtained by three dimensional atom probe (3DAP) and conventional TEM observations.

Fe-1.0wt%Cu alloy was prepared by arc melting followed by cold rolling. All samples were annealed at 825 °C for 4 h and subsequently quenched into ice water. Some of the samples were thermally aged at 525 °C for 20 min, 1, 10, and 100 h. In-situ tensile deformation experiments were performed at room temperature in a JEOL 4000FX TEM operating at 400 kV with a single tilt straining holder. The motion of dislocations was recorded by a CCD camera with a time resolution of 1/30 s. The slip planes had to be determined prior to measuring

bow-out angles of dislocation. Slip systems being activated were determined to be  $\langle 111 \rangle \{10\bar{1}\}$  or  $\{11\bar{2}\}$ .

Fig. 1 shows the typical morphology of dislocations during an in-situ TEM observation of Fe-1.0 wt % Cu after aging 20 min, 1 h, 10 h and 100 h at 525 °C. Dislocations are along  $\langle 111 \rangle$  direction and anchored at pinning points. Most of dislocations interacting with obstacles were of screw type. Copper precipitates were not observed by TEM after 20 min and 1 h aging, and were clearly observed at pinning points and in the matrix after 10 h and 100 h aging. The diameter was about 1 nm after 20 min and 1 h aging. They are considered to have a coherent b.c.c. structure after 20 min and 1 h aging. On the other hand, the precipitates were in the stage of transformation from b.c.c. structure to 9R structure, after 10 h aging. There is a peak in number density of copper precipitates at 1 h aging. Sometimes small defect clusters with a black dot contrast were observed to form during straining. These defect clusters are debris defects left after cross slips of dislocations.

The obstacle strength parameter,  $\cos(\varphi_c/2)$  was almost same after 20 min and 1 h aging. For increasing the aging times to 10 h and 100 h, the average obstacle strength increased with broader distributions. The obstacle strength depends on the precipitate diameter and “the impact parameter” which is the distance from the center of obstacle to a glide plane [3]. The relationship between the increase in shear stress and the increase in polycrystalline yield stress is given by following equation using the Taylor factor for polycrystals ( $M = 3.06$ ):

$$\sigma_y = \sigma_0 + \Delta\sigma_y = \sigma_0 + M\Delta\tau_c,$$

where  $\sigma_y$  is yield stress,  $\sigma_0$  is yield stress for Fe-1.0wt%Cu alloy as quenched without precipitation hardening. Fig. 2 shows a qualitative agreement between the yield stress measured by conventional tensile tests and that obtained from in-situ TEM observations.

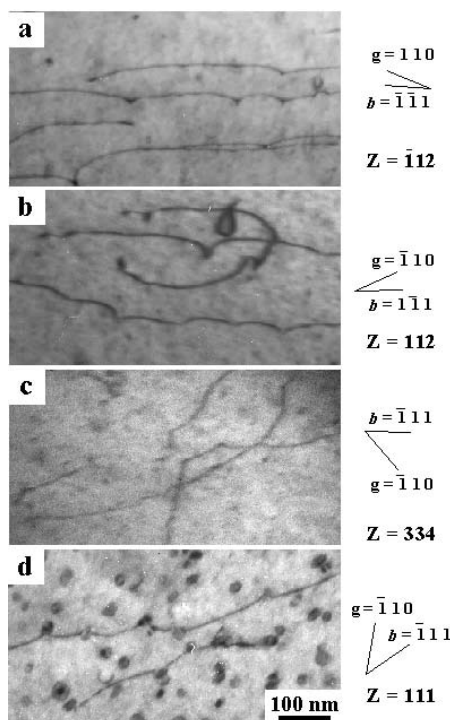


Fig. 1 The typical morphology of dislocations under stress during in-situ TEM observations in Fe-1.0wt%Cu aged 20 min (a), 1 h (b), 10 h (c) and 100 h (d) at 525 °C.

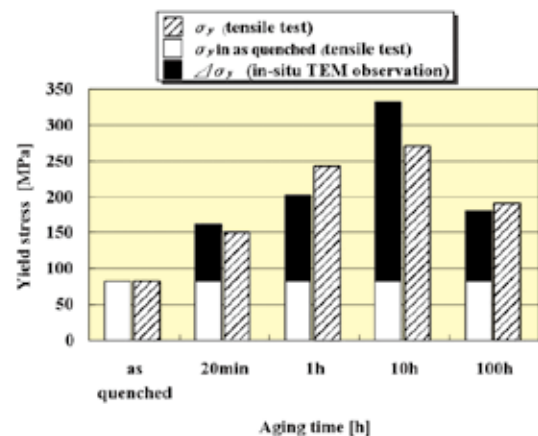


Fig. 2 Precipitate number density measured from 3DAP or TEM observation and estimated from in situ TEM observations. The yield stress measured from tensile tests and values calculated from the experimentally obtained microstructural data.

## References

- [1] K Nogiwa, N. Nita and H. Matsui, J. Nucl. Mater. in press.
- [2] K. Nogiwa, T. Yamamoto, K. Fukumoto, H. Matsui, Y. Nagai, K. Yubuta and M. Hasegawa, J. Nucl. Mater. **307-311**, 946 (2002).
- [3] T. Hatano and H. Matsui, Phys. Rev. **B72**, 094105 (2005).

## Contact to

Hideki Matsui (Nuclear materials engineering Division)  
e-mail: matsui@imr.tohoku.ac.jp

# Intrinsic Martensite Formation in Neutron Irradiated V-1.6%Y Alloys with Fine-grained Structure of Highly Pure Matrix

*It is known that in vanadium gaseous interstitials (H, N, O) cause transformation from the bcc to bct structure by elongating one axis relative to the other two to accommodate the induced strain. This paper describes the first finding of intrinsic martensite formation that is not associated with the interstitials for neutron irradiated V-1.6Y (in wt%) with a fine-grained structure of a highly pure matrix [1]*

Development of refractory transition metals with improved resistance against mechanical property degradation by high energy particle irradiation is required for their use under irradiation environments. It has been shown that the most effective microstructure to improve the radiation resistance consists of fine grains and finely dispersed particles, the finer the better because grain boundaries and particles can serve as effective sinks for irradiation induced point defects. For vanadium such a microstructural refinement requires a processing method that enables to make the vanadium matrix free from gaseous interstitials, particularly nitrogen and oxygen. This is because vanadium is chemically very reactive with the interstitials and their dissolution into the matrix leads to significant embrittlement. We have proposed an advanced powder metallurgical (P/M) method utilizing mechanical alloying and hot isostatic pressing and successfully developed ductile V-Y and V-Y-Cr alloys with fine grains of a highly pure matrix free from gaseous interstitials and very fine dispersoids of  $Y_2O_3$  and YN [2-4]. The  $Y_2O_3$  and YN dispersoids are formed as a result of consuming solute oxygen and nitrogen impurities.

V-1.6Y alloys were irradiated at 290 and 600°C to 0.25 and 0.6 displacement per atom (dpa), respectively, in the Japan Materials Testing Reactor to examine the effect of neutron irradiation. It has been demonstrated that the alloys exhibit much improved radiation resistance [5] Another noticeable finding is that the irradiated V-1.6Y exhibits the intrinsic martensite formation of a vanadium bct structure that is not caused by gaseous interstitials. The emergence of intrinsic martensite is the first to be observed in vanadium or its alloys not only in neutron irradiated states but also in unirradiated states. The main results and conclusions are as follows [1]:

1. The martensite emerges heterogeneously in some of the bcc grains of V-1.6Y and has a high density of  $\{101\}_{bct}$  microtwins as the lattice invariant shear strain. The bct structure exhibits a tetragonality ( $a/c$ ) of 1.06 as measured with Kikuchi line analyses.

2. The habit planes between the bct martensite and the surrounding bcc matrix are  $\{101\}_{bct} // \{110\}_{bcc}$ , which can be regarded as the close-packed plane with coherency even for the bct structure because of the slight changes in the lattice constants of both the phases.

3. The features of the P/M V-1.6Y alloys, an interstitial-scavenged matrix and extremely fine grains, are considered to be responsible for the martensite formation caused by irradiation.

4. The transformed vanadium bct lattice provides

preferential sites as the host phase for hydrogen atoms to occupy with an ordered arrangement (Fig. 1). The ordered arrangement of hydrogen atoms occurs in a very thin specimen area that is susceptible to hydrogen pickup associated with TEM specimen preparation after irradiation, but does not occur in a thicker specimen area.

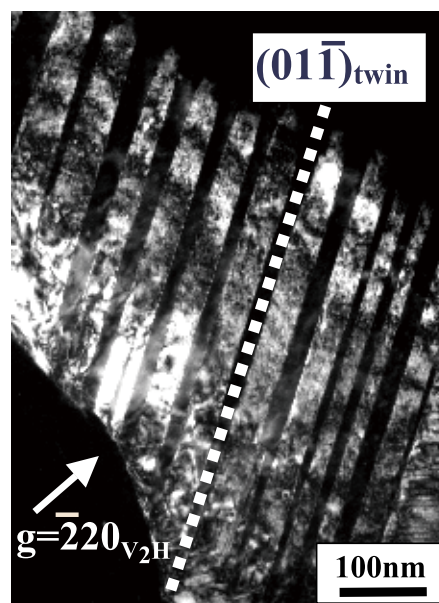


Fig. 1 TEM micrograph of dark field image from a very thin specimen area with a transformed region that provides preferential sites for hydrogen atoms to occupy with an ordered arrangements in V-1.6Y irradiated at 290°C to 0.25dpa.

5. The hydrogen content (H/V) in the ordered bct structure is estimated to be approximately  $H/V = 0.24$ . This content is much lower than  $H/V \sim 0.41$ , the lowest content of the  $\beta_1$  hydride phase that can exist in the thermoequilibrium state, supporting the absence of hydride formation in the bct phase.

## References

- [1] H. Kurishita, S. Kobayashi, K. Nakai, T. Kuwabara and M. Hasegawa, J. Nucl. Mater. **358**, 217 (2006).
- [2] T. Kuwabara, H. Kurishita and M. Hasegawa, J. Nucl. Mater. **283-287**, 611 (2000).
- [3] T. Kuwabara, H. Kurishita and M. Hasegawa, Mater. Sci. & Eng. A **417**, 16 (2006).
- [4] H. Kurishita, T. Kuwabara and M. Hasegawa, Mater. Sci. & Eng. A. **433**, 32 (2006).
- [5] H. Kurishita, T. Kuwabara, M. Hasegawa, S. Kobayashi and K. Nakai, J. Nucl. Mater. **343**, 318 (2005).

## Contact to

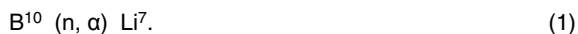
Hiroaki Kurishita (International Research Center for Nuclear Materials Science)

e-mail: kurishi@imr.tohoku.ac.jp

# Development Study of Fast Reactor Core with Hydride Neutron Absorber

We are now developing hafnium hydride control rods for Fast Breeder Reactor (FBR) in order to drastically prolong its in-core life accounting its superb characteristics of helium and swelling free features. A new hydride neutron absorber of nuclear reactor has proposed based on the results of irradiation experiments in Japan Materials Testing Reactor (JMTR) of Japan Atomic Energy Agency (JAEA). A metal-hydride has very high hydrogen atom density, which is equivalent to that of liquid water. Fast neutrons in nuclear reactors are efficiently moderated and are absorbed in the metal-hydride. The Hafnium hydride and Gd hydride are considered as neutron absorber in FBR.

Fast breeder reactor is considered as the major nuclear power source for the future. The B<sub>4</sub>C has been mainly used for control and shut down material in FBRs. But the life of B<sub>4</sub>C control rods is restricted by Pellet-Cladding Mechanical Interaction (PCMI) failure due to the He gas swelling of B<sub>4</sub>C pellet which is caused by the following nuclear reaction,



The concept how to prolong control rod life of FBR by using HfHx is illustrated in Fig. 1. In order to prolong the control rod life-time we propose to use HfHx as absorber material for FBR by the reasons that He gas is not generated in nuclear reaction of HfHx, and that HfHx can be expected to absorb neutron for more than 40 years owing to the fact that Hf<sup>178</sup> and Hf<sup>179</sup> which are generated by neutron captures of Hf<sup>177</sup> and Hf<sup>178</sup> respectively, also have large neutron capture cross sections which are expressed by the following reaction,.

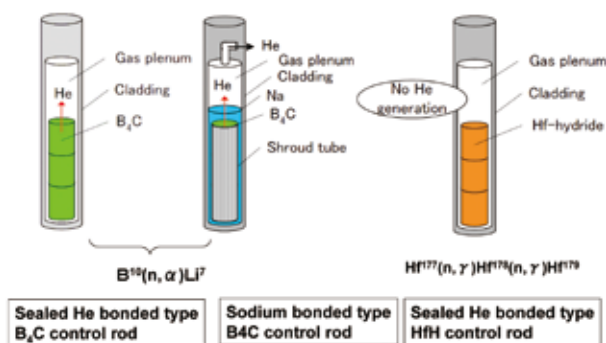


Fig. 1 Schematic of HfHx application concept to FBR control rod.

The control rod assembly, which contains Hf-hydride, is considered to enhance neutron absorption in fast reactors. In general, a metal-hydride has very high hydrogen atom density, which is equivalent to that of liquid water. Fast neutrons in nuclear reactors are efficiently moderated and are absorbed in the metal-hydride. As the ratio of H to Hf increases, the Hf-control rod can more efficiently absorb neutrons in fast reactor core. For example, the worth of HfH<sub>1.0</sub>

is larger than that of B<sup>10</sup> 40% enriched B<sub>4</sub>C.

One of the most important R&D items to establish the idea of Hf-hydride control rod is the development of Hf-hydride pellet, which can be safely irradiated for long time. The idea has proposed based on the results of irradiation experiments in JMTR of JAEA. Fig. 2 shows the structure of capsule for irradiation experiments, where the actinide hydride pellet were loaded. After irradiations, non-destructive examinations (X-ray photograph, gamma scanning and so on) and destructive examinations (electron microprobe analysis, physical property measurements and so on) were performed and the integrity of the hydride pellet during irradiation was assured.

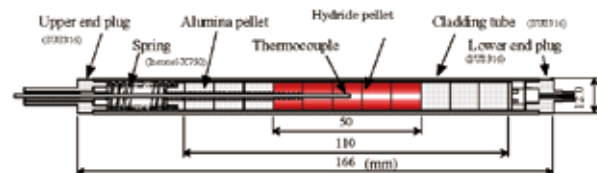


Fig. 2 Schematic of HfHx application concept to FBR control rod.

The development program of hydride neutron absorber has been started, which is accepted as an innovative nuclear research and development program of Ministry of Education, Culture, Sports, Science and Technology of Japan.

## References

- [1] K. Konashi et al., "Development of advanced control rod of hydride hafnium for fast reactor", Proc. of the ICAPP2006, Reno, USA (2006).
- [2] K. Konashi et al., "Study on application of hafnium hydride control rods to fast reactors", Proc. of the 15th Pacific Basin Nuclear Conference, Sydney, Australia (2006).
- [3] K. Konashi and M. Yamawaki, "The development of thorium hydride fuel", Characterization and quality control of nuclear fuels edited by Ganguly C. and Jayaraj R.N., 92, Allied Publishers Pvt. Ltd. (2004).

## Contact to

Kenji Konashi (International Research Center for Nuclear Materials Science)

e-mail: konashi@imr.tohoku.ac.jp

## Defect Structure of Nonstoichiometric Plutonium Oxide

*Nuclear fuel systems typically require decades to optimize, since the assessment of behavior of nuclear fuel is made based on empirical data and irradiation testing. As a general trend, it is tried to assess them on basic scientific understanding. In this work, an oxygen defect of plutonium oxide has been studied by the first principle calculations, which predict the electron structure of materials without experimental data.*

Plutonium, which is generated in an operating nuclear reactor due to transmutation of uranium, is one of important materials as nuclear fuel. Plutonium is mainly used in the nuclear reactor in the chemical form of oxide. Plutonium oxide has a wide range of non-stoichiometry, determined by temperature and oxygen partial pressure. Non-stoichiometric plutonium oxide is represented by  $\text{PuO}_{2-x}$ , where  $x$  is non-stoichiometry. The oxygen partial pressure is a key parameter, which controls chemical reactions in the fuel pin.

It is very important to develop a model, which is able to predict well the correlation between the non-stoichiometry of  $\text{PuO}_{2-x}$  and the partial pressure of oxygen. In the design of nuclear fuel, the model based on defect chemistry has been used for calculation of oxygen potential. The defect chemistry model is essentially empirical one, since the parameters in the defect chemistry model are adjusted by the experimental data. In this study, the first principle calculations were used to check the validity of the defect chemistry model.

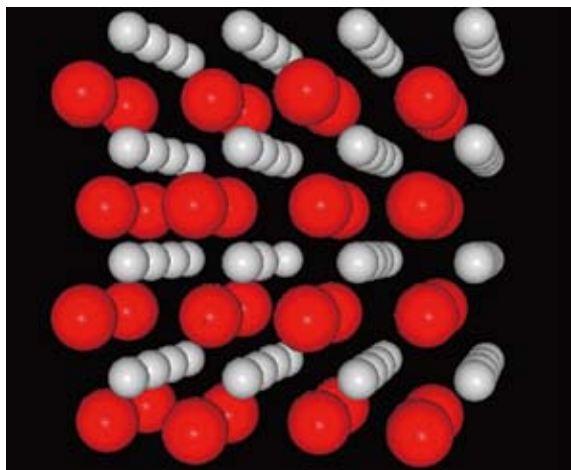


Fig.1 Supercell for plutonium oxide with oxygen defect. Red and white spheres indicate plutonium and oxygen atoms, respectively.

The total energy and the electronic structure of  $\text{PuO}_{2-x}$  have been calculated by PAW method within the GGA. We also used the DFT+U methodology to check localization of f-electron. Figure 1 shows a supercell of 96 atoms containing 32 plutonium atoms, 63 oxygen atoms and one oxygen vacancy. The calculations were performed with the HITACHI/SR-8000 in Tohoku University. The calculated lattice parameter and the enthalpy of formation of plutonium dioxide are in good agreement with the experimental values. The

vacancy formation energy, which was defined as the energy required for extraction of an oxygen atom from the perfect lattice, was calculated to be 4.20eV. This value is close to that calculated from the experimental data.

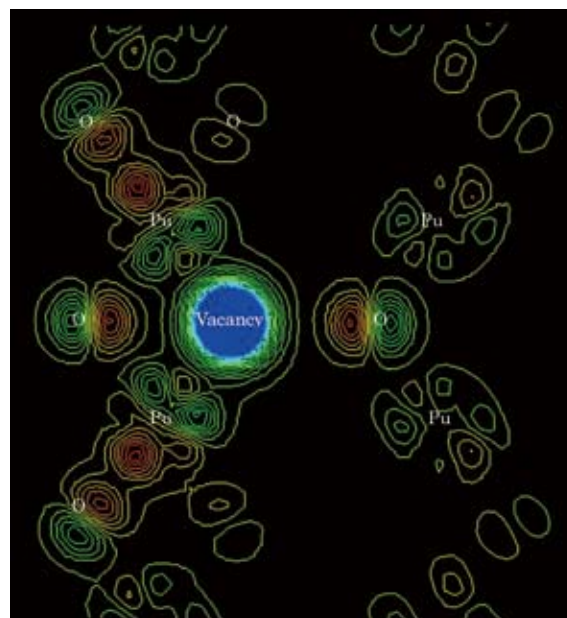


Fig. 2 Differential charge densities near oxygen vacancy

Difference in the charge density between the defect model and the perfect model has been calculated to make the effect of vacancy clear (Fig. 2). The six nearest neighbor oxygen atoms moved from original site toward the oxygen vacancy site. The two atoms of those were shown in Fig. 2. It is also shown that the charge densities around the two nearest neighbor plutonium atoms are affected by the oxygen vacancy. The calculation results show that only the nearest neighbor plutonium atoms are affected by the oxygen vacancy. This agrees with the following picture used in the classical defect chemistry, that is, the oxygen has two electrons provided by plutonium, which are left behind when an oxygen atom is leaving lattice position. These two electrons are localized on two plutonium atoms, turning  $\text{Pu}^{4+}$  into  $\text{Pu}^{3+}$ .

### References

- [1] K. Konashi, H. Matsui, Y. Kawazoe, M. Kato and S. Minamoto, J. Phys. Soc. Jpn. **75** suppl., 143 (2006).
- [2] K. Konashi, M. Kato, S. Minamoto, 'First Principle Plane-Wave Pseudopotential Calculation of Point Defects in  $\text{PuO}_{2-x}$ ', ANS 2005 Winter Meeting, Nov. 15-19, 2005, Washington, D.C., USA

### Contact to

**Kenji Konashi** (International Research Center for Nuclear Materials Science)  
e-mail: [konashi@imr.tohoku.ac.jp](mailto:konashi@imr.tohoku.ac.jp)